

## Supporting Information

### **Interconnected NiCo<sub>2</sub>O<sub>4</sub> nanosheet arrays grown on carbon cloth as host, adsorber and catalyst for sulfur species enabling high-performance Li-S batteries**

Junli Zhou <sup>a</sup>, Xiaolan Yang <sup>a</sup>, Yajun Zhang <sup>a</sup>, Jinzhu Jia <sup>a</sup>, Xinjian He <sup>a</sup>, Lin Yu <sup>a, \*</sup>, Yuede Pan <sup>b,c,\*</sup>, Jingwen Liao <sup>d</sup>, Ming Sun <sup>a</sup>, Jun He <sup>a</sup>

<sup>a</sup> Key Laboratory of Clean Chemistry Technology of Guangdong Higher Education Institutions, Guangzhou Key Laboratory of Clean Transportation Energy Chemistry, Faculty of Chemical Engineering and Light Industry, Guangdong University of Technology, Guangzhou 510006, Guangdong, China. \*E-mail: gych@gdut.edu.cn;

<sup>b</sup> Institute of Energy Innovation, College of Materials Science and Engineering, Taiyuan University of Technology, Taiyuan 030024, China. \*E-mail: panyuede@tyut.edu.cn;

<sup>c</sup> Key Laboratory of Advanced Energy Materials Chemistry (Ministry of Education), College of Chemistry, Nankai University, Tianjin 300071, China.

<sup>d</sup> Chinese Academy of Sciences, Guangzhou Institute of Advanced Technology, Guangzhou 511458, Guangdong, China.

\* Corresponding author.

E-mail addresses: gych@gdut.edu.cn (Lin Yu); panyuede@tyut.edu.cn (Yuede Pan)

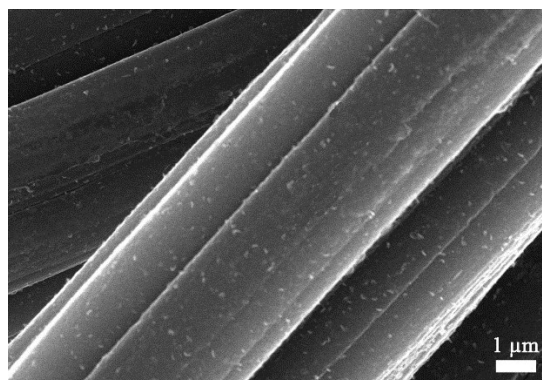


Figure S1. SEM image of bare CC.

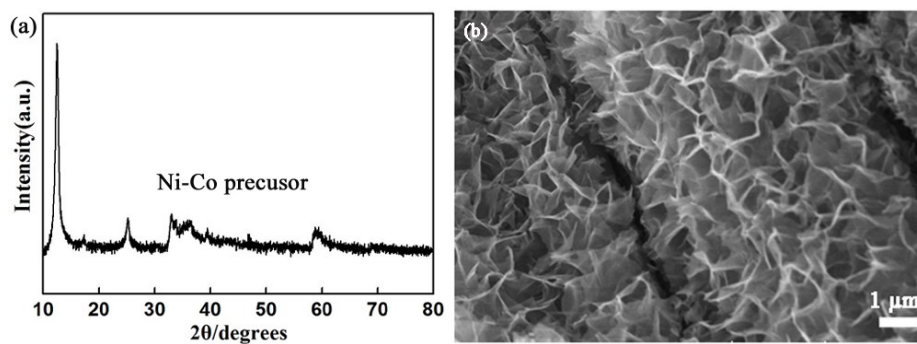


Figure S2. XRD pattern (a) and SEM image (b) of the precursor of  $\text{NiCo}_2\text{O}_4/\text{CC}$ , with a composition of  $(\text{Ni}_x\text{Co}_y)(\text{OH})_a(\text{CO}_3)_b(\text{H}_2\text{O})_c$ .

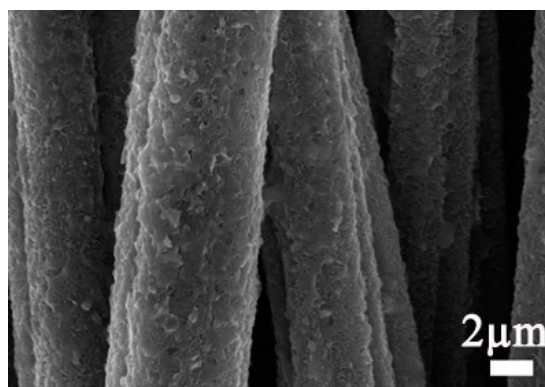


Figure S3. FESEM images of S/CC with sulfur loading of  $1.15 \text{ mg cm}^{-2}$ .

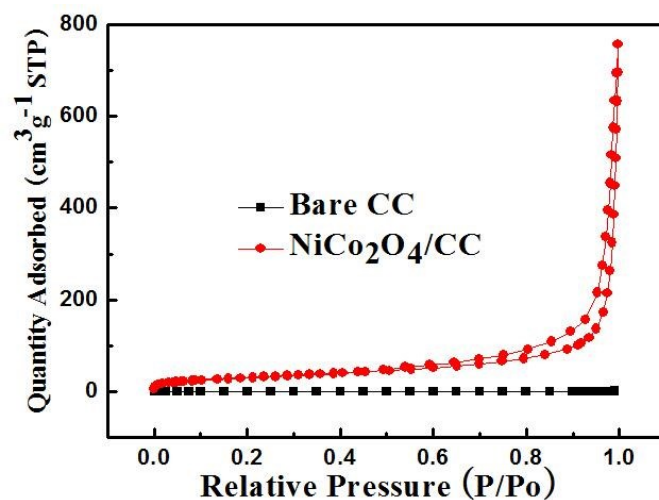


Figure S4. N<sub>2</sub> adsorption-desorption isotherms of bare CC and NiCo<sub>2</sub>O<sub>4</sub>/CC.

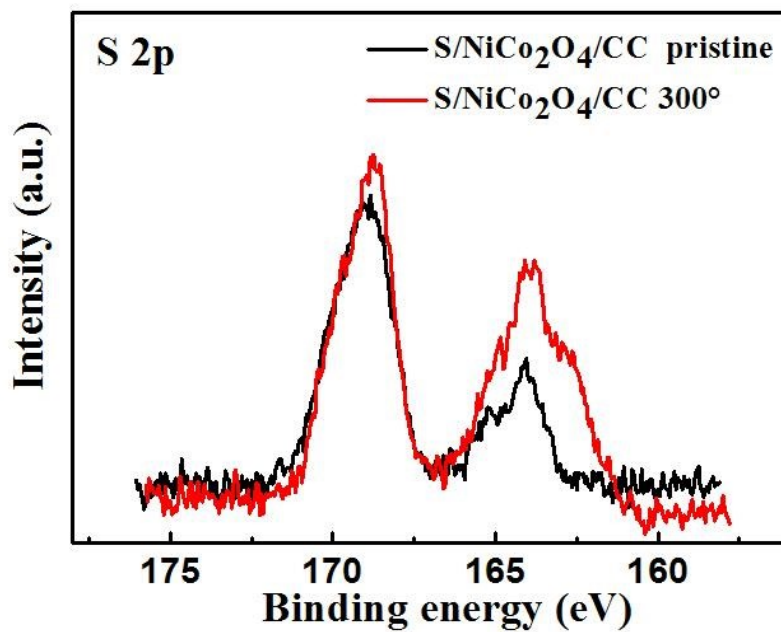


Figure S5. High-resolution S 2p XPS spectra of S/NiCo<sub>2</sub>O<sub>4</sub>/CC before and after 300°C treatment.

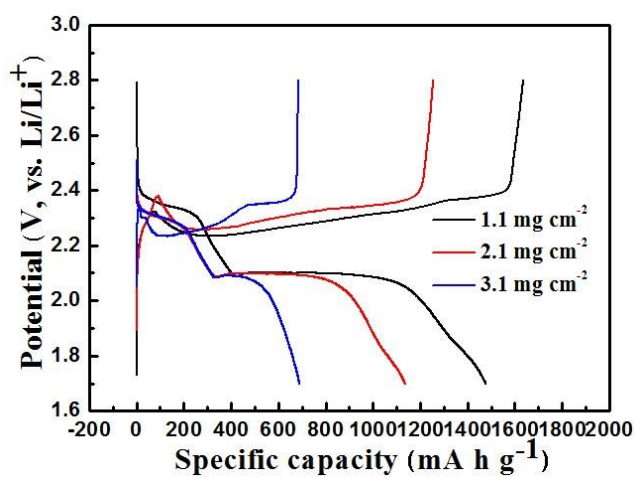


Figure S6. The first charge-discharge profiles at 0.1 C for S/NiCo<sub>2</sub>O<sub>4</sub>/CC cathodes with varied sulfur loading.

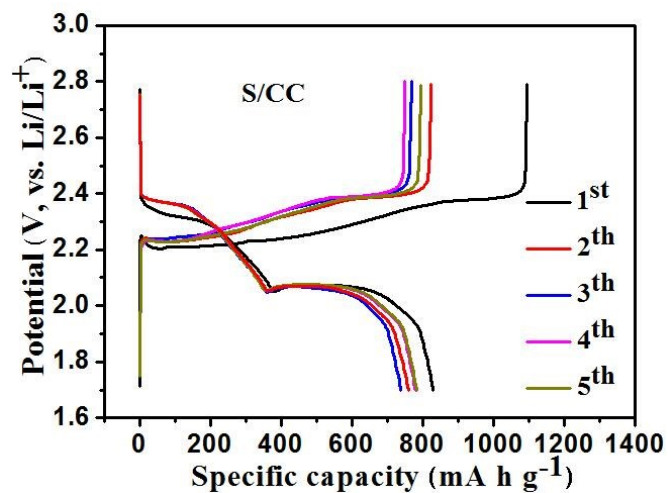


Figure S7. Charge-discharge profiles for the first five cycles at 0.5 C for S/CC. The initial Coulombic efficiency is lower than 80%.

$$I_p = (2.69 \times 10^5) n^{1.5} A D^{0.5} C v^{0.5} (25 \text{ }^\circ\text{C})$$

Randles-Sevcik equation for lithium ion diffusion process, where  $I_p$  is the peak current (A),  $n$  is charge transfer number,  $A$  is the electrode area ( $\text{cm}^2$ ),  $D$  is the lithium ion diffusion coefficient ( $\text{cm}^2 \text{ s}^{-1}$ ),  $C$  is the concentration of Li ions ( $\text{mol cm}^{-3}$ ), and  $v$  is the scan rate ( $\text{V s}^{-1}$ ).

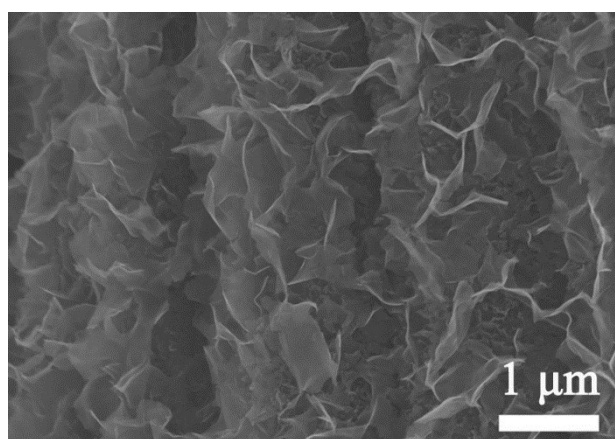


Figure S8. SEM image of S/NiCo<sub>2</sub>O<sub>4</sub>/CC electrode after 400 cycles.

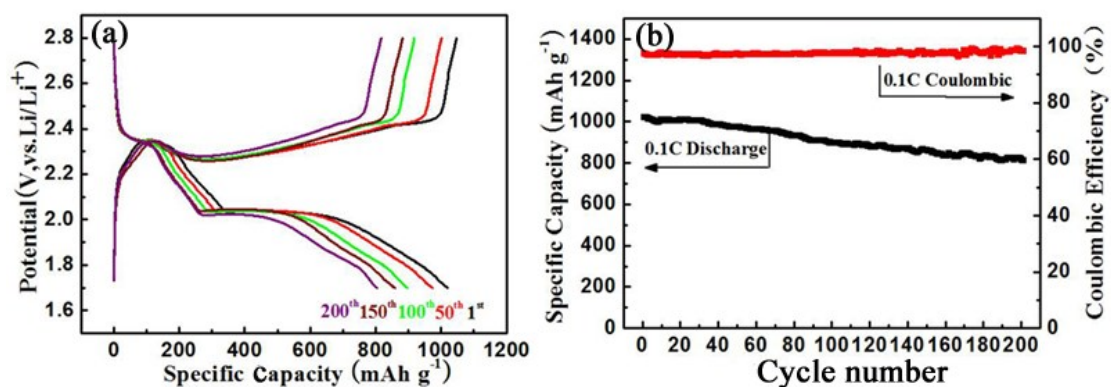


Figure S9. (a) Charge-discharge profiles during cycling at 0.1 C for S/NiCo<sub>2</sub>O<sub>4</sub>/CC (sulfur loading: 2.73  $\text{mg cm}^{-2}$ ) at the 1<sup>st</sup>, 50<sup>th</sup>, 100<sup>th</sup>, 150<sup>th</sup> and 200 cycles. (b) Cycling performances and Coulombic efficiencies of S/NiCo<sub>2</sub>O<sub>4</sub>/CC (sulfur loading: 2.73  $\text{mg cm}^{-2}$ ) at 0.1 C.

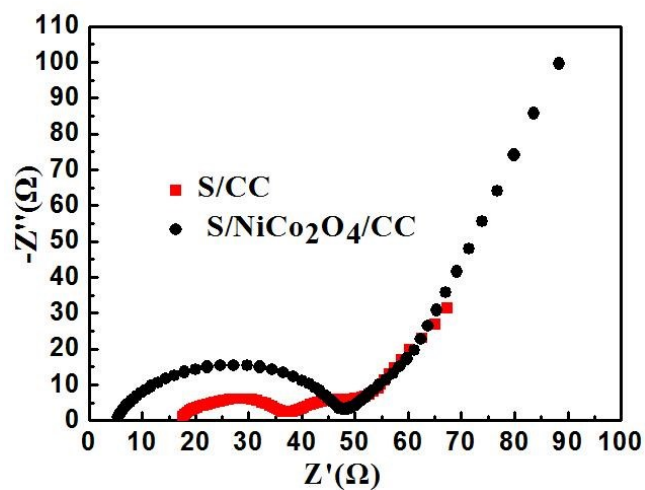


Figure S10. EIS measurements for S/CC and S/NiCo<sub>2</sub>O<sub>4</sub>/CC after cycling at 100% of charge state.

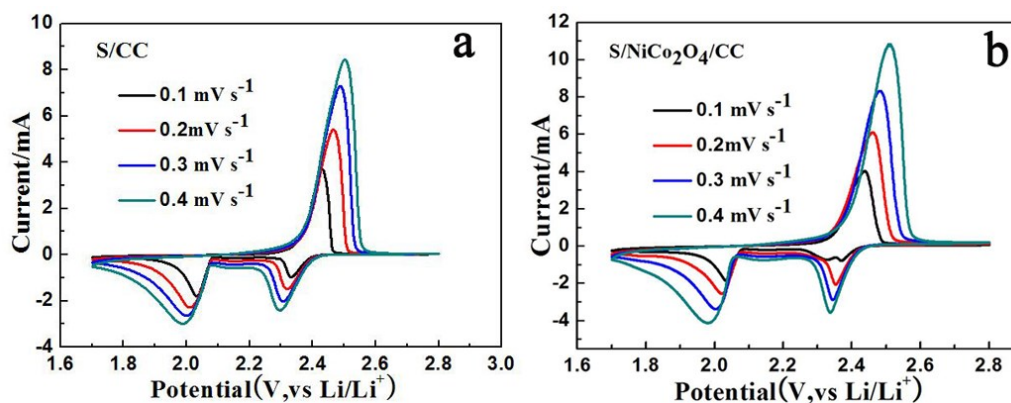


Figure S11. CV curves for (a) S/CC and (b) S/NiCo<sub>2</sub>O<sub>4</sub>/CC composites at different scan rates from 0.1 to 0.4 mV s<sup>-1</sup>.

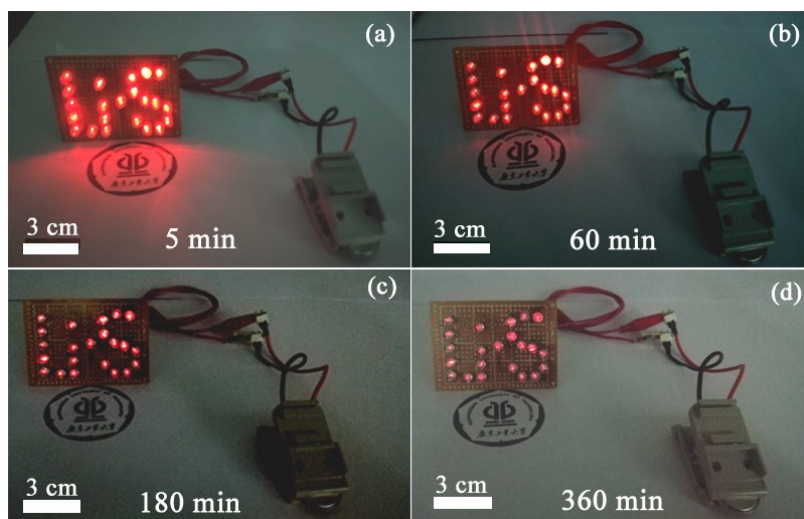


Figure S12. Demonstration of a Li-S coin cell with the S/NiCo<sub>2</sub>O<sub>4</sub>/CC electrode in illuminating red LED for (a) 5 min, (b) 60 min, (c) 180 min, (d) 360 min.